KINEMATIC EVIDENCE FOR DIFFERENT PLANETARY NEBULAE POPULATIONS IN THE ELLIPTICAL GALAXY NGC 4697

Niranjan Sambhus
Astronomisches Institut, Universität Basel, Venusstrasse 7, 4012 Binningen, Switzerland

Ortwin Gerhard
Current address: Max-Planck Institut für Extraterrestrische Physik, Giessenbachstrasse, D-85748 Garching, Germany and
Astronomisches Institut, Universität Basel, Venusstrasse 7, 4012 Binningen, Switzerland

Roberto H. Méndez
Institute for Astronomy, University of Hawaii, 2680 Woodlawn Drive, Honolulu, HI 96822, USA
Accepted for publication in Astronomical Journal

ABSTRACT

We have analysed the magnitudes, kinematics and positions of a complete sample of 320 PNs in the elliptical galaxy NGC 4697. We show (i) that the PNs in NGC 4697 do not constitute a single population that is a fair tracer of the distribution of all stars. The radial velocity distributions, mean velocities, and dispersions of bright and faint subsamples differ with high statistical confidence. (ii) Using the combined data for PNs brighter than 26.2, we have identified a subpopulation of PNs which is azimuthally unmixed and kinematically peculiar, and which thus neither traces the distribution of all stars nor can it be in dynamical equilibrium with the galaxy potential. (iii) The planetary nebula luminosity functions (PNLF) of two kinematic subsamples in NGC 4697 differ with 99.7% confidence, ruling out a universal PNLF. We estimate that the inferred secondary PN population introduces an uncertainty in the bright cutoff magnitude of ~ 0.15 mag for this galaxy. – We argue that this secondary PN distribution may be associated with a younger, $\gtrsim 1$ Gyr old stellar population, perhaps formed in tidal structures that have now fallen back onto the galaxy, as has previously been suggested for the X-ray point sources in this galaxy, or coming from a more recent merger/accretion with a red galaxy. The use of PNs for extragalactic distance determinations is not necessarily compromised, but their use as dynamical tracers of dark halos will require deep observations and careful analysis of large PN samples.

Subject headings: elliptical galaxies:kinematics– individual(NGC 4697)–galaxies: kinematics and dynamics– galaxies: distances and redshifts–planetary nebulae: general

1. INTRODUCTION

Planetary Nebulae (PNs) have become increasingly important in extragalactic astronomy, for distance determinations via their luminosity function (LF) (Jacoby 1989; Ciardullo et al. 1989; Jacoby, Ciardullo, Ford 1990; Méndez 1999; Ferrarese et al. 2000; Ciardullo 2003, and references therein), as kinematic tracers of the dark halos of galaxies (Arnaboldi et al. 1998; Saglia et al. 2000; Méndez et al. 2001; Romanowsky et al. 2003), and as tracers for the distribution and kinematics of the diffuse stellar population in galaxy clusters (Feldmeier, Ciardullo, & Jacoby 1998; Feldmeier et al. 2004; Arnaboldi et al. 2002, 2004; Gerhard et al. 2005). Due to their strong narrow line emission at [OIII]λ5007, PNs can be easily detected out to distances beyond 20 Mpc with narrow-band photometry and slitless spectroscopy (Feldmeier, Ciardullo, & Jacoby 1998; Arnaboldi et al. 2002; Méndez et al. 2001; Douglas et al. 2002), and to ~ 100 Mpc with multi-slit imaging spectroscopy (Gerhard et al. 2005). Moreover, they are observed in elliptical and spiral galaxies, making them an indispensible tool to support distances obtained by other

methods (such as Cepheids, Surface brightness fluctuations, the Tully-Fisher relation, SNe Ia), and to measure the kinematics of stellar populations whose surface brightness is too faint for absorption line spectroscopy.

For distance determination the Planetary Nebulae Luminosity Function (PNLF) is normally modeled as having a universal shape that depends only on the absolute bright magnitude cutoff $M^\star$:

$$N(M) \propto e^{0.307M}(1 - e^{3(M^\star - M)}), \qquad (1)$$

where $N(M)$ is the number of PNs with absolute magnitude M (Ciardullo et al. 1989). Observationally, the cutoff magnitude $M^\star$ has a quasi-universal value of -4.5 with only a weak dependence on host galaxy metallicity expressed by the system's oxygen abundance, and which can be compensated for by a quadratic relation in [O/H] (Dopita et al. 1992; Ciardullo et al. 2002). In practice, the PN magnitudes $m(5007)$, after correcting for the interstellar reddening, are fitted to the model PNLF of eq. 1 convolved with the photometric error profile, yielding a value of the distance modulus (Ciardullo et al. 1989). The absence of any systematic variations in $M^\star$ and the PNLF shape has been verified in galaxies with significant population gradients, and among galaxies of different morphologies within galaxy clusters/groups up to Virgo (Jacoby 1997; Ciardullo 2003, and references

Electronic address: sambhus@astro.unibas.ch
Electronic address: gerhard@mpe.mpg.de
Electronic address: mendez@ifa.hawaii.edu

therein).

This universality of the PNLF and the cutoff magnitude $M^\star$ must be considered surprising, given that the PN luminosity in the [OIII]λ5007 line depends on the mass and metallicity of the central star, as well as on the electron gas temperature, optical thickness and dust extinction of the surrounding nebula. Indeed, some current semi-analytic simulations of the PNLF seem to be at odds with the observational trends. Méndez et al. (1993); Méndez & Soffner (1997) indicate small possible dependencies of $M^\star$ on the total size of the PN population, on the time elapsed since the last episode of star formation, and on how optically thin the PNs are; concluding, however, that only careful studies would detect such effects in the observed PNLF. In contrast, more recent PNLF simulations by Marigo et al. (2004) contradict the observed narrow spread in $M^\star$ and predict large variations of several magnitudes depending on a variety of realistic star formation and evolution scenarios. So is the PNLF truly quasi-universal and its cutoff magnitude nearly independent of population age and metallicity?

PNs are also important as test particles to study the kinematics and dark matter distribution in the halos of elliptical galaxies. Since the PN population is expected to arise from the underlying galactic stellar distribution, their radial velocities can be used as effective kinematic tracers of the mass distribution. However, the required PN sample sizes are many 100s (Merritt & Saha 1993), or at least 100 or more in conjunction with absorption line spectroscopy, which has limited this application to only a few nearby galaxies (Hui et al. 1995; Arnaboldi et al. 1998; Saglia et al. 2000; Méndez et al. 2001; Romanowsky et al. 2003; Peng, Ford & Freeman 2004). In recent simulations of disk galaxy mergers involving dark matter, stars, and gas, Dekel et al. (2005) predict that the young stars formed in the merger have steeper density profiles and larger radial anisotropy than the old stars from the progenitor galaxies, and they argue that if the PNs observed in elliptical galaxies were to correspond to the young population rather than to all stars in the simulations, their velocity dispersion profile would match the measured dispersion profiles of Romanowsky et al. (2003). So do PNs really trace the stars and their kinematics in elliptical galaxies?

Different stellar populations may have, and in general would have, different phase-space distributions in the same galaxy potential. The simplest approach for dynamical modelling, taking the PN velocities as a random sampling of the stellar velocities, is however valid only when the PN population properties and their kinematics are uncorrelated. Except in special cases this also requires that the PNLF is independent of the stellar population. Vice-versa, if there existed differences in the PNLF or the bright cutoff magnitude for different stellar populations, they would best be identified by studying the correlations between PN magnitudes and kinematics or positions of these tracers, in a single galaxy where all PNs are at the same distance.

In this paper, we report on such a study in the elliptical galaxy NGC 4697, an excellent target for this purpose because of the large sample of PN velocities known from Méndez et al. (2001). Our analysis shows the existence of distinct PN populations which differ in their kinematics, brightnesses, and spatial distributions. This suggests

that the answer to both the questions posed above may be 'no' – in general, different stellar populations may have slightly different PNLFs, and the observed PN population in elliptical galaxies may not be a fair tracer of their stars. The paper is organised as follows: in § 2 we review the properties and PN data of this galaxy and discuss the magnitude and velocity completeness of our sample. Our statistical analysis of these data is given in § 3 where we demonstrate the inhomogeneity of the sample in the space of velocities, magnitudes, and positions. §§ 4,5 conclude our work, giving also a brief discussion of its implications.

2. NGC 4697: PROPERTIES AND PN SAMPLE

NGC 4697 is a normal, almost edge-on E4-5 galaxy located along the Virgo southern extension. From the multi-colour CCD photometry of Goudfrooij et al. (1994), the effective radius is $R_{eff} = 95''$, the mean ellipticity is 0.45, and the PA is constant, consistent with a near-axisymmetric luminosity distribution. Isophotal analysis shows that this galaxy has a positive $a4$ coefficient suggesting a disk-like structure within $0.6R_{eff}$ (Carter 1987; Scorza & Bender 1995).

From optical spectroscopy, its dominant stellar population has an age of $\sim$ 9 Gyr (Trager et al. 2000), consistent with the red mean B-V=0.91 colour. Stellar absorption line kinematics along the major axis (PA 66°) of NGC 4697 have been reported by Binney, Davies & Illingworth (1990) and Dejonghe et al. (1996); these velocity data can be well described by dynamical models based on the luminous mass distribution only.

Méndez et al. (2001) detected and measured radial velocities of 531 PNs extending out to $300''(\sim 3R_{eff})$ in this galaxy, with observational errors of $\sim$ 40 km s^{-1}. Via dynamical analysis, they determined a constant mass to light ratio $\Upsilon_B = 11$ within $\sim 300''$, which is consistent with a 10 Gyr old stellar population with a Salpeter mass function and slightly super solar metallicity.

X-ray observations with ROSAT (Sansom, Hibbard & Schweizer 2000) show only small amounts of hot gas in the halo of this galaxy. Using more recent *Chandra* data, Sarazin, Irwin & Bregman (2000) could resolve most of the X-ray emission into nonuniformly distributed X-ray binary point sources (XPS), suggesting that NGC 4697 has lost most of its interstellar gas. Though NGC 4697 does not show any signature of recent interactions, Zezas et al. (2003) present evidence that the distribution of these X-ray sources is inconsistent with the optical morphology of NGC 4697, and propose that these sources are mostly high mass X-ray binaries (HMXBs) associated with young stellar populations related to fallback of material in tidal tails onto a relaxed merger remnant, or to shock-induced star formation along tidal tails. They estimate typical fallback times of such tidal tails to be much longer than the settling timescale of the remnant and expect similar results for other elliptical galaxies with populations of $\sim$ 10 Gyr age.

For the work in this paper we use the PN sample presented by Méndez et al. (2001). After removing the possible contaminants and unclear detections, they report unambiguous detection of 535 PNs. However only 526 out of 535 PNs have confirmed measurements of velocity

and magnitude, and we use these in our analysis. In order to determine the PNLF, it is crucial to estimate the magnitude where PN detection incompleteness sets in. Detectability of a PN varies with the background galaxy surface brightness; for a statistically complete sample the surface number density of PNs should be directly proportional to it. Méndez et al. (2001) show that their PN sample is statistically complete down to $m(5007) = 27.6$ magnitudes outside an elliptical region of semi-major axis $60''$. In our analysis, we have thus defined two data sets: a *Complete sample* (with PNs brighter than 27.6, outside the central ellipse of semi-major axis $60''$), and a *Total sample* (consisting of all PNs with measured magnitude and radial velocity). The total number of PNs in these data sets is 320 and 526, respectively.

The systemic velocity (V_{sys}) of NGC 4697, obtained by averaging the observed velocity of all 526 PNs is $1274 \, km \, s^{-1}$, which agrees with the values quoted in the literature (Méndez et al. 2001, and references therein). The on-band filter configuration used to detect and measure velocities of these PNs has a peak wavelength of 5028 Å, peak transmission of 0.76, equivalent width of 48.5 Å, and FWHM of 60 Å (Méndez et al. 2001). The FWHM corresponds to a velocity range of $\pm 1800 \, km \, s^{-1}$ around the systemic velocity of NGC 4697. Thus the filter transmission width is large enough to facilitate observations of PNs with all velocities bound to NGC 4697, irrespective of their magnitude. Indeed, even at magnitudes as faint as $m(5007) = 28$ in the Total sample, PNs with large velocities $\sim 300 \, km \, s^{-1}$ are detected. Thus the velocity coverage in both samples (Total and Complete) is not biased with respect to the PN magnitudes.

The PN magnitudes were measured by Méndez et al. (2001) from their undispersed images; they are accurate to 0.1 and 0.2 mag for $m(5007)$ brighter and fainter than 26.5, with systematic effects below 2%. As a further test relevant for the present work, Méndez et al. (2001) used the redundancy provided between their E and W fields: plotting magnitude differences between the two measurements (E and W) of PN candidates as a function of difference in distance from the center of the CCD, they found a scatter diagram without any evidence of correlation. Méndez et al. (2001) estimated the errors in the PN velocities from calibration, image registration, spectrograph deformation and guiding errors to be $40 \, km \, s^{-1}$. The velocities of 165 PNs were measured independently in the E and W field of Méndez et al. (2001); these velocities agree within a standard deviation of $36 \, km \, s^{-1}$. In order to check whether a systematic difference between the velocities of bright and faint PNs could be introduced by an asymmetric PSF (a possibility suggested by K. Freeman), we have superposed the PSF's of three groups of 10 of the brightest PNs, one selected at random, and two selected among those PNs with the highest and lowest radial velocities. In the three cases we estimated the shift of the centroid of the entire PSF with respect to the centroid of the upper part. The shifts were smaller than $10 \, km \, s^{-1}$, and in some cases they were in the opposite sense compared to the results discussed below.

3. THE DISTRIBUTION OF NGC 4697 PNS IN VELOCITY, MAGNITUDE, AND POSITION

In this Section, we search for stellar population effects in the kinematics of the PNs in NGC 4697, by analysing

the Total and Complete data sets with respect to their three observables: velocity, magnitude and position. For both data sets, we convert the observed PN radial velocities into co-rotating or counter-rotating velocities, as follows. With the galaxy center at the origin of the reference frame, and the X-axis oriented along the major axis (PA= 66 deg), the absorption line stellar-kinematic data predict positive line-of-sight mean velocity with respect to the galaxy systemic velocity, at slit positions towards the South-West of the center with X coordinate > 0, and vice versa. We denote this sense of rotation as *co-rotating*, and the opposite sense as *counter-rotating*. By definition, the major axis absorption line data is *co-rotating*.

3.1. *Sub-populations of PNs in the velocity–magnitude plane*

After subtracting the systemic velocity from the PN radial velocities, we define reduced velocities $U = (V - V_{sys}) * sign(x)$ and denote the PNs with $U > (<) \, 0$ as co-rotating (counter-rotating). By definition, the major axis absorption line data have $U > 0$. The resulting values of U are displayed against the observed magnitudes in Figure 1. Even at magnitudes as faint as $m(5007) = 28$ in the Total sample, PNs with large velocities $\sim 300 \, km \, s^{-1}$ are detected, showing that there is no kinematic bias at faint magnitudes. Henceforth, unless stated otherwise, we will always use the Complete sample for our analysis.

Figure 1 shows that the Complete PN sample appears to exhibit a correlation between magnitudes and kinematics, with faint PNs showing more co-rotation than bright PNs. We have performed several statistical tests to verify the significance and look for the origin of this correlation. Table 1 shows the results of Pearson's r-test for correlated data. Velocities of counter-rotating PNs are strongly linearly correlated with their brightness, while those of co-rotating PNs are almost independent of their magnitude distribution. Further, we divided our sample into 3 equal magnitude bins each of size $\Delta m = 0.7$, hereafter referred to as *faintest*, *intermediate*, and *brightest PNs*, and computed the mean reduced velocity and its dispersion in each of these bins along with the significance of their differences. As shown in Table 2, the *faint* and *bright PN subsamples* defined through these bins have different mean reduced velocity and dispersions at 94% and 99.3% confidence, respectively. In Figure 2 we have plotted the cumulative velocity distribution of PNs in the brightest and faintest magnitude bins. There is a visible excess of bright PNs with counter rotating velocities. It is particularly evident from this figure that the brightest counter rotating PNs display a velocity distribution that differs from the rest of the PNs from the Complete sample with high confidence.

Thus it is clear that the observed correlation between the PNs kinematics and their magnitudes is compelling, and it arises because the faintest and brightest PNs have significantly different velocity distributions. There appears to exist an additional component of bright, counter-rotating PNs with respect to the overall sample.

3.2. *Spatial Distribution*

If these correlations have a physical origin, they should also be manifest in the spatial distribution of these
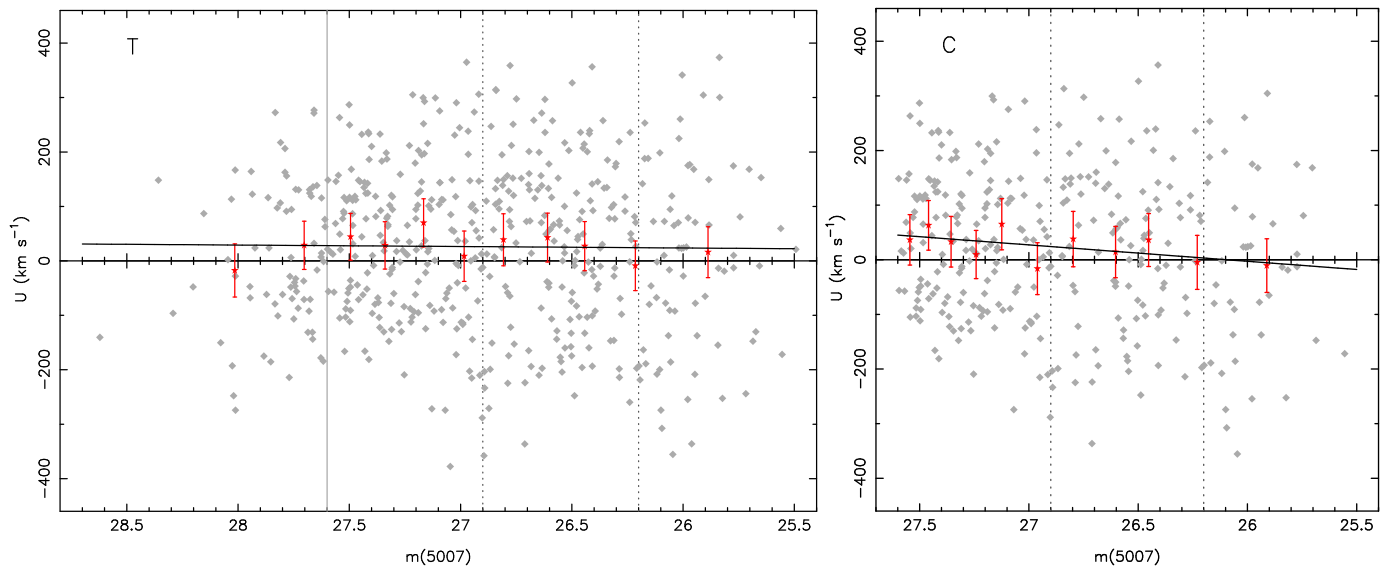
FIG. 1.— PN reduced velocity U versus magnitude plots for the Total (T) and Complete (C) samples. Reduced velocities have been *folded* such that positive (negative) velocity denotes co- (counter-) rotating PNs. Red stars (with error bars) are mean U values of PNs binned in magnitude such that each bin contains 30 (50) data points in the Complete (Total) sample. The error bars include the sample variance in the bin and the velocity errors ($40\,\mathrm{km\,s^{-1}}$) added in quadrature. The black solid lines are least square linear fits to this binned data. In both samples, PNs with $m(5007) \lesssim 26.5$ have mean $U \approx 0$. The dotted vertical lines separate the Complete sample into 3 bins, each of size 0.7 magnitude (see text). The Complete data set shows a linear correlation between $m(5007)$ and U: Fainter PNs show more co-rotation than their brighter counterparts. In the Total sample, the vertical solid line at $m(5007) = 27.6$ denotes the limiting magnitude, though not all PNs brighter than this magnitude constitute the Complete sample.

	r	$\mathcal{P}_{\mathrm{r}}$
All	0.12	3.1×10^{-2}
Co-rot	-3.5×10^{-2}	0.64
Counter-rot	0.24	5.8×10^{-3}

TABLE 1

PEARSON'S r-TEST FOR LINEAR CORRELATION OF PN MAGNITUDES WITH REDUCED VELOCITY U, FOR THE ENTIRE COMPLETE SAMPLE, THE CO-ROTATING, AND THE COUNTER-ROTATING SUBSAMPLES. VALUES OF r CLOSE TO ±1 INDICATE A STRONG LINEAR CORRELATION; VALUES CLOSE TO 0 INDICATE LITTLE OR NO CORRELATION. $\mathcal{P}_{\mathrm{r}}$ IS THE PROBABILITY THAT TWO UNCORRELATED VARIABLES WOULD GIVE THE r-COEFFICIENT AS LARGE AS OR LARGER THAN THE MEASURED ONE, FOR A NORMAL DISTRIBUTION OF r. SMALL VALUES OF $\mathcal{P}_{\mathrm{r}}$ IMPLY SIGNIFICANT CORRELATION.

PNs. Thus we now enquire whether the PN kinematics and magnitudes depend on their spatial location in the galaxy.

In Figure 3 we plot the spatial locations of all the 526 PNs in this galaxy. The central incompleteness ellipse is also displayed. PNs brighter than $m = 26.2$ (which is 0.71 magnitude deeper than the brightest PN) are shown as filled blue squares (co-rotating) and filled red triangles (counter-rotating). Inside the incompleteness ellipse, the distribution of the bright PNs appears to be concentrated around an elliptical annulus. However, we did not find

	$\overline{U}$ (error)	σ	t	$\mathcal{P}_t$	F	$\mathcal{P}_F$
$m(5007) \geq 26.9$	32.9 (9.5)	123.1				
			1.92	6.0×10^{-2}	1.84	7.4×10^{-3}
$m(5007) \leq 26.2$	-20.0 (25.8)	167.3				

TABLE 2

MEAN REDUCED VELOCITY ($\overline{U}$) AND DISPERSION (σ) OF BRIGHTEST AND FAINTEST PNs, ALONG WITH THE RESULTS FROM STUDENT t-TEST AND F-TEST. VERY SMALL VALUES OF $\mathcal{P}_t$ AND $\mathcal{P}_F$ IMPLY THAT THE DIFFERENCES BETWEEN THE OBSERVED $\overline{U}$ AND σ ARE STATISTICALLY SIGNIFICANT.

any kinematic evidence (like a rotation curve signature) relating these bright PNs to the central stellar disk: either they are not physically related to the disk, or the evidence from the data is inconclusive.

Outside the incompleteness ellipse, the distribution of bright PNs does not follow the surface brightness of the host galaxy: there is a significant left-right asymmetry, with more bright PNs to the right side of the galaxy minor-axis (27 ± 5) than to the left side (15 ± 4). Méndez et al. (2001) discuss at length the possible differences in their E (east) and W (west) fields, and are convinced that the maximum systematic errors in the measured photometry, positions and radial velocities are below 2%, $0''.06$ and $20\,\mathrm{km\,s^{-1}}$, respectively. Hence we conclude that the left-right asymmetry in number counts of bright PNs is not affected by detection uncertainties.

Subsequently, we carried out several tests to check whether the brightest and faintest, or the co- and counter-rotating PNs are distributed differently in the galaxy. It turns out that the radial PN distribution is independent of their sense of rotation. However, the distribution of PN distances from the galaxy mid-plane differs for co- and counter-rotating PNs at a confidence level of 73%.

The left-right asymmetry is confirmed by inspecting the azimuthal distribution of the faint and bright PNs. In the literature we found a related analysis by Zezas et al. (2003) who compared the azimuthal distribution of *Chandra* X-ray point sources (XPS) with the optical surface brightness of NGC 4697. We follow their PA convention, and plot the cumulative angular distributions of the bright, intermediate, and faint PNs in our Complete sample in Figure 5. For comparison, the right panel of Fig. 2 from Zezas et al. (2003) is also shown. The angular distribution of all PNs in the Complete sample has a shape somewhere in between that of the XPS and that of the optical light. The brightest PNs are in
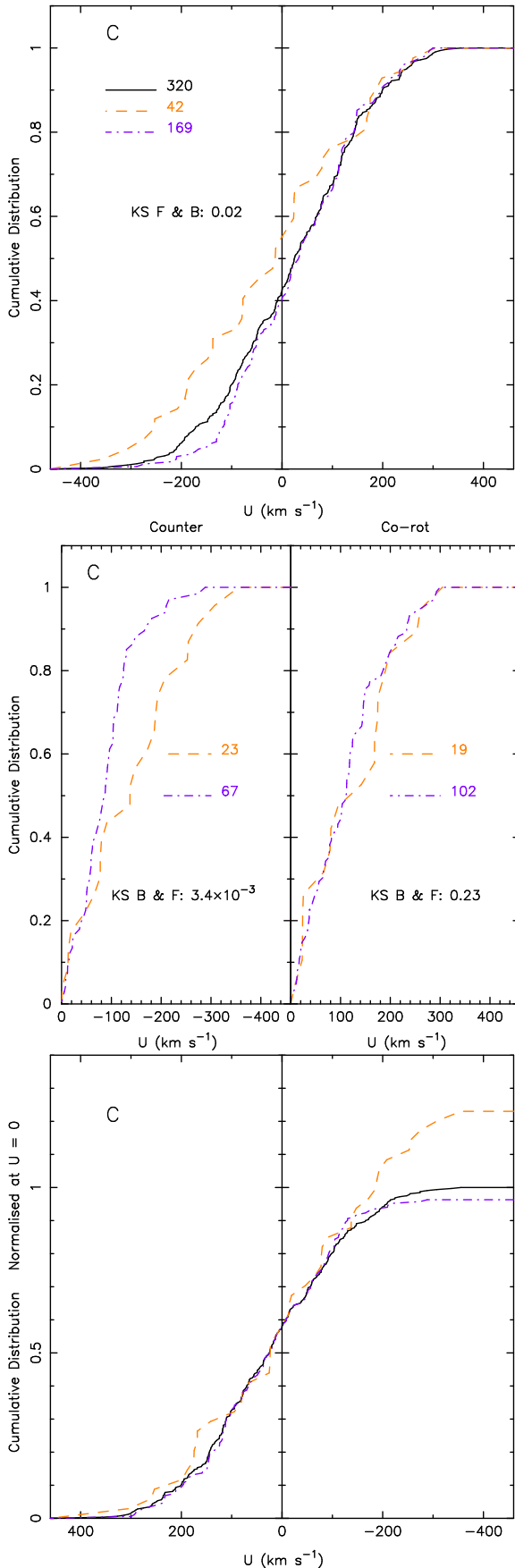
FIG. 2.— Cumulative velocity distribution of brightest PNs ($m \leq$ 26.2, orange dashed line), faintest PNs ($m \geq$ 26.9, purple dashed-dotted line), and the entire Complete sample (black solid line). The entire velocity range is shown in the top panel. In the middle panel the velocities are divided according to their sense of rotation. The bottom panel shows the cumulative distribution (shown from $+ve$ to $-ve$ values), normalised at $U = 0$. The Kolmogorov Smirnov probabilities show that the brightest counter rotating PNs have
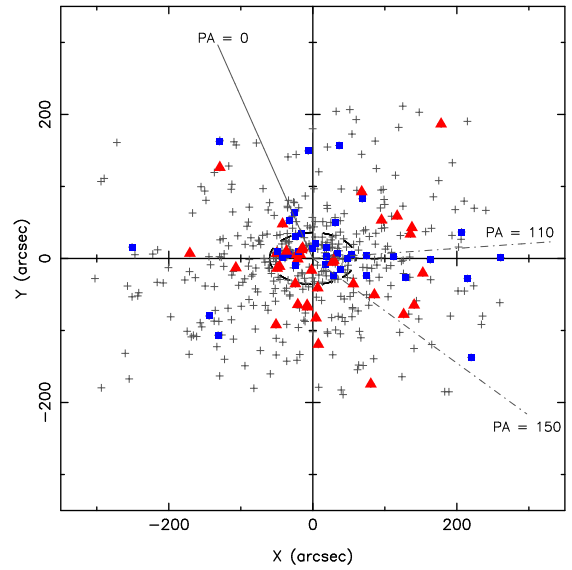
FIG. 3.— Spatial distribution of 526 PNs in NGC 4697 (plus-symbols). PNs brighter than 26.2 are shown as filled blue squares (co-rotating) and filled red triangles (counter-rotating). The dashed ellipse denotes the central incompleteness region. The left-right asymmetry in the distribution of bright PNs is apparent. The true North direction is shown as a solid line along PA = 0°. Following Zezas et al. (2003), we measure the azimuth from this direction in the clock-wise sense. Two special directions PA = 110° and 150° are shown as dash-dotted lines (see text).
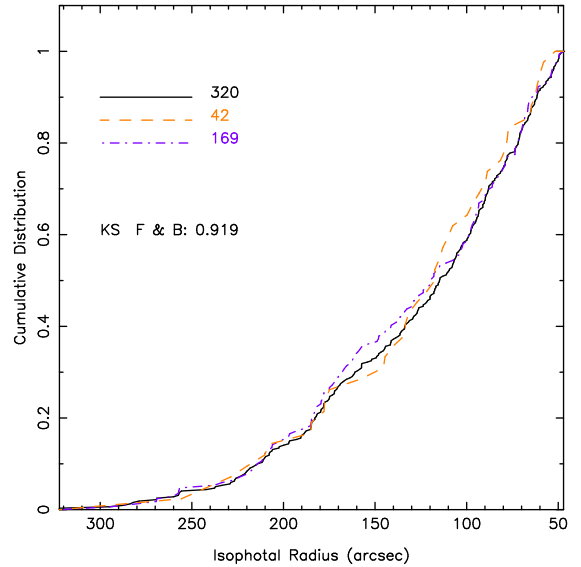

FIG. 4.— Cumulative radial distributions of all PNs in the Complete sample (solid black line), the bright subsample (dashed orange line), and the faint subsample (purple dash-dotted line). The KS probability shows that these are all consistent with one another.

complete disagreement with either of these distributions; they seem to be more concentrated in a narrow angular sector between $110° \lesssim$ PA $\lesssim 150°$ (see Fig. 3), with only 1.9% probability that the faint and bright PN subsamples are drawn from the same azimuthal distribution. At the same time, the radial distribution of the faint and bright subsamples are not significantly different (Figure 4).

The velocity distribution of the brightest PNs is also correlated with their azimuthal distribution. In Figure 6 we plot the mean radial velocity and its dispersion in angular sectors containing approximately constant number
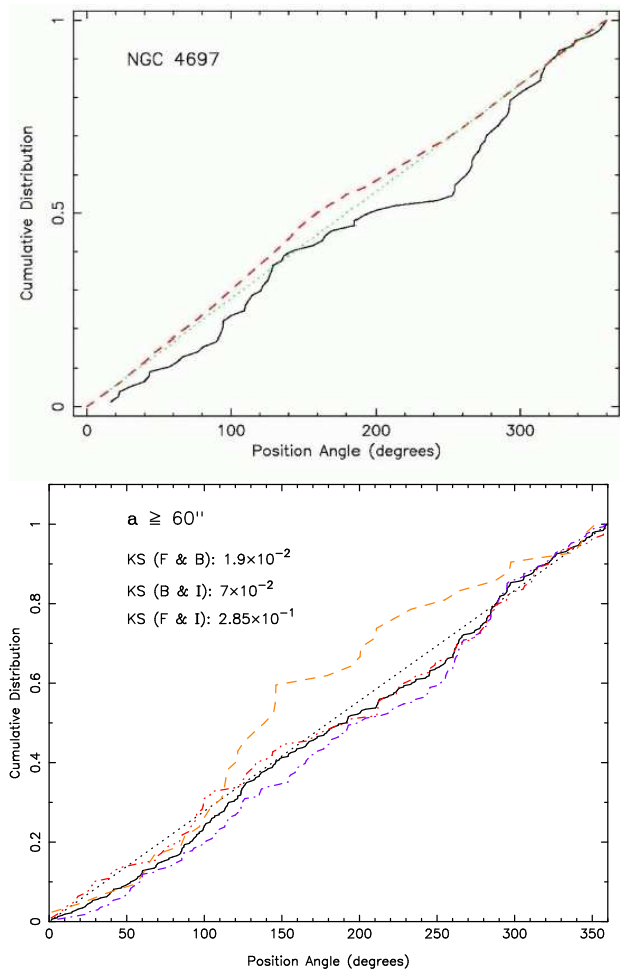
Fig. 5.— Azimuthal distribution of discrete sources in NGC 4697. *Top:* Cumulative distribution of azimuths of X-ray point sources (black solid line), adapted from Zezas et al. (2003). The green dotted line is for a uniform distribution, while the red dashed line shows the azimuthal distribution of the galaxy optical light (in R-band). *Bottom:* PNs in the brightest, intermediate, and faintest bins as defined in § 3.1 are shown by the orange dashed line, the red dash-triple dotted line, and the purple dash-dotted line, respectively. All PNs in the Complete sample are shown by the solid black line. Note the large increase in the distribution of bright PNs and the moderate increase in the distribution of intermediate PNs, relative to the faint PNs, at PA $\sim 110°$ (see text for details). The KS probability of the faintest and brightest PNs being drawn from the same underlying distribution is only 1.9%, while the intermediate PNs are still compatible with the faint PNs (KS probability 28%).

of PNs from the bright subsample, as well as an angular running average of their mean radial velocity. Along both sides of the major-axis of the galaxy, the brightest PNs have positive velocity, while showing a relatively low velocity dispersion, perhaps due to infall as suggested for the XPS by Zezas et al. (2003). Along the minor-axis they have a large dispersion with a mean velocity that is negative. This kinematics is compatible with neither the faint PN velocities nor the stellar absorption line data. On the other hand, the fainter PNs show a regular azimuthal distribution in the mean line-of-sight radial velocity and velocity dispersion. Note that their velocity dispersion is in the mean smaller than that of the bright sample. The kinematics of the intermediate luminosity PNs is intermediate between those of the bright and faint subsamples. The intermediate luminosity PNs thus con-
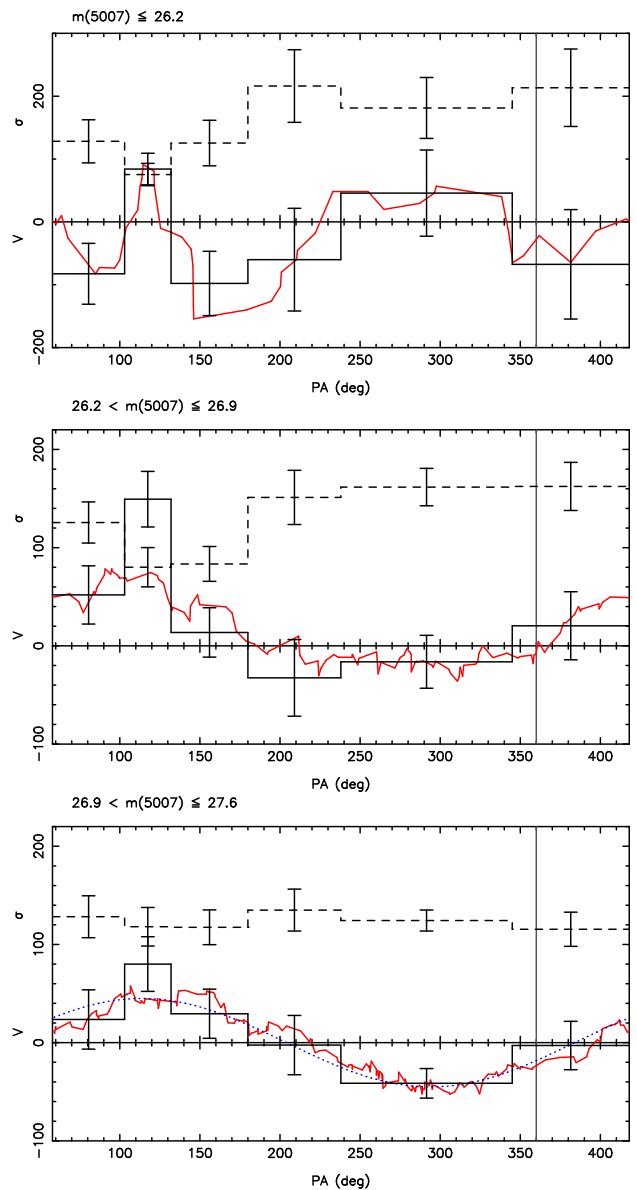

Fig. 6.— Azimuthal distributions of PN velocities. The PA is measured clockwise from North, as in the convention of Zezas et al. (2003), so that the galaxy major axis is along PA $= 114°, 294°$. Solid (dashed) histograms show the mean velocity (dispersion) and their errors in different angular bins. The red ragged lines show running averages of mean velocity. *Top:* Velocities of PNs brighter than $m(5007) = 26.2$ in the Complete sample. Bin sizes are chosen so as to have approximately constant number of PNs (~ 7) in each bin. The mean velocity along the major (minor) axis is positive (negative) on both sides of the center. The running average is also over 7 PN velocities. The velocity dispersion is largest (smallest) on the minor (major) axis. *Middle:* Velocities of PNs with $26.2 < m(5007) \leq 26.9$ in the same angular bins as in the top panel. The running average is over 27 PNs. *Bottom:* Velocities of PNs with $26.9 < m(5007) \leq 27.6$ in the same angular bins as in the top panel. The faint PNs show a rotation pattern as for the absorption line data but with a smaller peak velocity, and are consistent with a flat dispersion of $\sim 120 \, \mathrm{km \, s^{-1}}$. The running average is over 33 PNs. The blue dotted line shows a sinusoidal fit. The kinematics of the intermediate brightness PNs is intermediate between the faint and bright PNs.
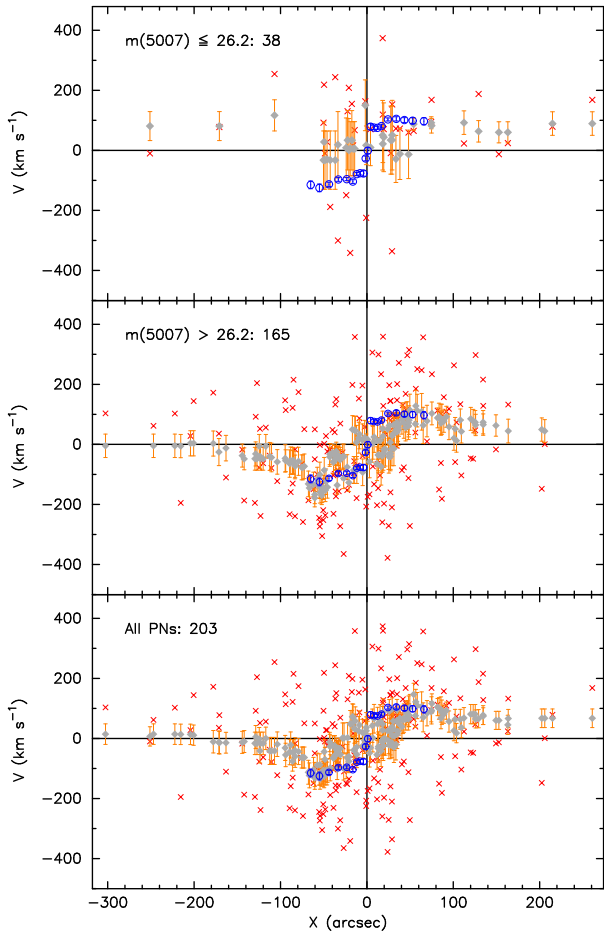
FIG. 7.— Velocity within ±30" of the major axis for bright and faint/intermediate PNs separated at $m(5007) = 26.2$. Blue circles show stellar absorption line spectroscopy (ALS) data from Binney, Davies & Illingworth (1990), red crosses are individual PN velocities, and grey diamonds are near neighbour running averages. The faint/intermediate sample is in approximate agreement with the ALS data, while the bright sample has a velocity consistent with zero within R_{eff} and positive velocities on both sides of the galaxy center.

tain significant contributions from both of the different populations that dominate the bright and faint bins, respectively.

Furthermore, including the bright PNs in deriving kinematics for the whole PN sample introduces significant contamination effects. In Figure 7, we demonstrate this by plotting the mean PN velocities along a $±30"$ wide slit about the major-axis. The PNs have been separated into faint/intermediate and bright sub-samples at $m(5007) = 26.2$. Inside the R_{eff}, the mean velocities of the faint PNs agree with stellar absorption line spectroscopic (ALS) data from Binney, Davies & Illingworth (1990), while the bright PNs have much smaller mean velocities, consistent with ~ 0. In the outer parts, the velocity asymmetry in the bright PNs leads to a positive mean velocity on both sides of the galaxy center. Both the faint/intermediate sample and the entire PN sample also show some asymmetry: the outer mean velocities on the $X < 0$ side reach zero, but not the negative values expected from reflecting the positive values at $X > 0$. This confirms that also the intermediate/faint subsample contains a fraction of PNs stemming from the out-of-equilibrium population traced by the bright PNs.

However, the streaming velocity of the majority of the faint PNs does appear to decrease on both sides of the center. Similarly contaminated results could be expected for the derived velocity dispersions.

Several important conclusions can be drawn from these figures. (i) The bright PNs as defined in Section 3.1 and Fig. 1 do not trace the azimuthal distribution of light in NGC 4697. (ii) They do not trace the fainter PNs in their azimuthal kinematics; thus, a large fraction of them must belong to a separate PN subcomponent originating from a separate stellar population. (iii) Third, they are not in dynamical equilibrium in the gravitational potential of NGC 4697. (iv) Because this subpopulation does not trace the stars, including its PN velocities into dynamical analysis of the galaxy will lead to significant errors in the results.

3.3. *Kinematic dependence of PNLF*

What can we learn about the luminosity functions of the two kinematic components of the PN system in NGC 4697? The cumulative magnitude distributions of the co-rotating and counter-rotating subsamples in Fig. 1 have only 28% KS probability of stemming from the same distribution (top panel of Figure 8). However, the fact that there are both co-rotating and counter-rotating bright PNs in the bright sample whose azimuthal distribution is unmixed, shows that counter-rotation is not a *clean* discriminator after all for the secondary population of PNs in NGC 4697. Thus the luminosity functions of the main and secondary PN populations in this galaxy may be a lot more different than this figure of 28% would suggest.

From Fig. 6 we estimate that the main population of PNs in NGC 4697 has a mean radial velocity $\overline{v}_{faint} \simeq 45 \, \text{km s}^{-1} \sin(\text{PA} - 24°)$, with a dispersion of $\sigma_{faint} \simeq 120 \, \text{km s}^{-1}$, so its reduced mean velocity is $0 < \overline{U}_{faint} \lesssim 45 \, \text{km s}^{-1}$. Thus in the bottom panel of Fig. 8 we show the cumulative magnitude distribution of the PNs in the velocity range $-100 \, \text{km s}^{-1} \leq U \leq 200 \, \text{km s}^{-1}$ and compare it with the cumulative distribution of the PNs with $U < -100 \, \text{km s}^{-1}$. These velocity ranges are dominated by the main and secondary PN populations in the sample, respectively. Now the Kolmogorov Smirnov significance test shows that the magnitude distributions from these sections of Fig. 1 have only probability 0.3% of being drawn from the same distribution. This result is strong enough to imply that the PNLF cannot be universal – the PNLF in NGC 4697 depends on a kinematic selection.

In the following, we will use the velocity range $-100 \, \text{km s}^{-1} \leq U \leq 200 \, \text{km s}^{-1}$ as an approximate kinematic selection criterion for the main PN population in NGC 4697. The luminosity function of the strongly counter-rotating PNs in Fig. 1 – a first approximation to the luminosity function of the secondary PN population in NGC 4697 – differs from that of the main PN distribution so defined in the sense that it contains more bright PNs near the cut-off and fewer faint PNs than the main population (see Fig. 8). Now an important question is: in what proportion do both populations contribute to the brightest PNs, and do they have different cutoff magnitudes?
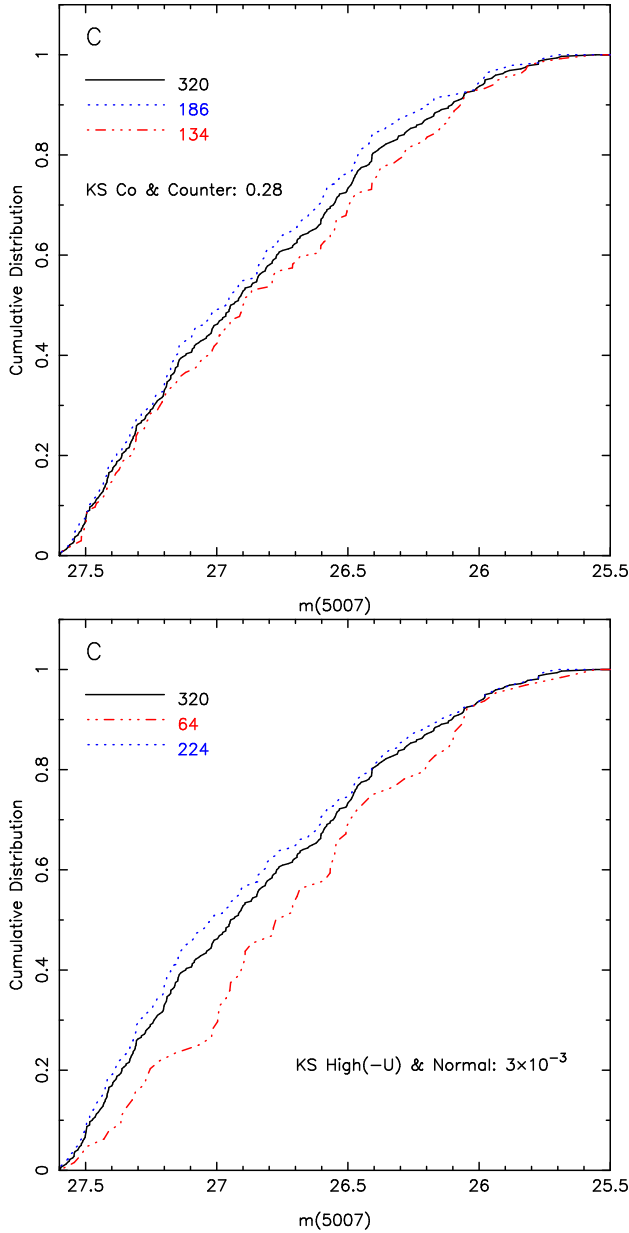
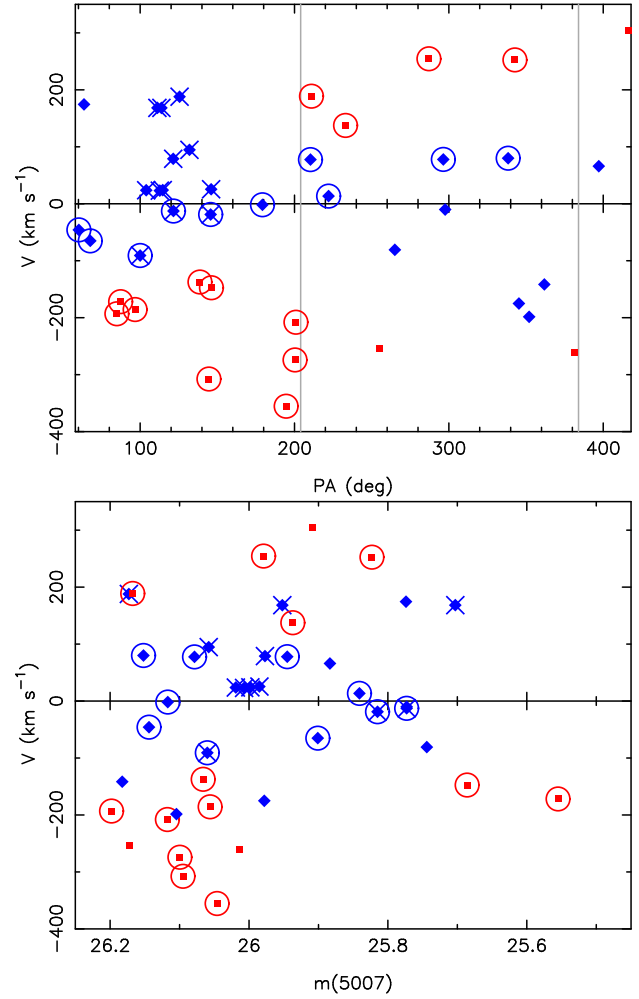To investigate this, we show in Figure 9 the veloci-

Fig. 9.— Disentangling the bright PN subsample from radial velocities, luminosities, and position angles on the sky. *Top:* Radial velocity – position angle plane. Red squares (blue diamonds) show PNs whose reduced velocities are outside (within) $-100\,\mathrm{km\,s^{-1}} \leq U \leq 200\,\mathrm{km\,s^{-1}}$. Circled symbols denote counter-rotating PNs; many of these are kinematic outliers. The two grey lines denote the position angle of the minor axis. The distribution of blue diamonds is approximatively uniform in PA except near PA= $100° - 150°$ where there are 12 PNs (crossed diamonds) instead of the expected 2 PNs. *Bottom:* Radial velocity – magnitude plane. The symbols are as in the top panel. 6/8 of the brightest PNs are either kinematic outliers or are found in the overdense angular region.

Fig. 8.— *Top:* Cumulative distributions of PNs magnitudes for all (black solid line), co-rotating (blue dotted line) and counter-rotating (red dash-dotted line) PNs in NGC 4697. The magnitude distribution of co- and counter-rotating PNs is similar with only 28% probability. *Bottom:* Cumulative magnitude distributions of the main PN sample ($-100\,\mathrm{km\,s^{-1}} \leq U \leq 200\,\mathrm{km\,s^{-1}}$, blue dotted line) and the extreme counter-rotating sample ($U < -100\,\mathrm{km\,s^{-1}}$, red dash-dotted line) defined in the text, along with that of the total sample (black solid line). The first two luminosity functions are different with 99.7% confidence; thus the PNLF cannot be universal.

ties, magnitudes, and position angles of the entire bright PN subsample (see Figs. 1 and 6). The top panel shows (i) that 13/16 of the bright PNs, whose radial velocities differ most from those of the faint population, are counterrotating. This explains the differences between the velocity distributions of co- and counter-rotating PNs that first suggested more than one PN population in Section 3.1. (ii) Also, even in the kinematically normal bright PNs, there is a large overdensity (10/12) in the angular range PA= $100° - 150°$. The bottom panel shows in addition that many of the brightest PNs are either

kinematic outliers or found in the angular overdensity (6/8).

Clearly, to arrive at a main population of NGC 4697 PNs that is in dynamical equilibrium in the gravitational potential, we must remove the angular overdensity. Then we are left with 16 PNs in the range $-100\,\mathrm{km\,s^{-1}} \leq U \leq 200\,\mathrm{km\,s^{-1}}$ of a total bright subsample of 42 PNs; however, there is some freedom in the way the angular overdensity is removed. In the following, we explore two assumptions: (i) using all 12 PNs in the angular overdensity, but weighting each one by $2/12 = 0.17$, and (ii) removing the brightest 10 of the 12 PNs in the overdensity. The resulting luminosity functions for both cases are plotted in Figure 10; they differ only slightly.

Thus in the following we use the kinematic condition $-100\,\mathrm{km\,s^{-1}} \leq U \leq 200\,\mathrm{km\,s^{-1}}$ together with assumption (ii) above to ensure azimuthal uniformity of the bright PNs, as an improved selection criterion for PNs in

the main population in NGC 4697. We keep all PNs in the intermediate luminosity bin with $-100\,\mathrm{km\,s^{-1}} \leq U \leq 200\,\mathrm{km\,s^{-1}}$, because Fig. 5 showed that their azimuthal asymmetry is not large. Also, we have checked that the mean angular velocity distribution in this magnitude bin after applying the kinematic selection follows approximately the sinusoidal variation of the faint PNs, and the velocity disperion is approximately constant. The resulting main population sample is identified by their brightness, distribution and kinematic properties.

Comparing the luminosity function in Figure 10 of this main PN population, with the luminosity function of all PNs in NGC 4697, we see that the bright cutoff of the main population is shifted to fainter magnitudes. We note that the bright cutoff could be shifted further to fainter magnitudes if some of the kinematically normal and azimuthally uniform bright PNs were also part of the secondary population, which we cannot tell from the present data.

We can ask now what is the effect, in practice, on the PNLF distance determination. The reduced sample for the main PN population in NGC 4697 has 214 objects. After binning these data into 0.2 mag intervals, we transform the apparent magnitudes $m(5007)$ into absolute magnitudes, adopting the extinction correction of 0.105 mag (Méndez et al. 2001) and assuming different distance moduli, and we compare the results with the PNLF simulations of Méndez & Soffner (1997). This is the same procedure used in Méndez et al. (2001) for the PNLF distance determination. The comparison is shown in Fig. 11. We conclude that the PNLF distance modulus should be increased slightly from 30.1 (the earlier determination based on the full sample) to 30.2 or 30.25. For comparison, the χ^2-fit to the same data (blue line in Fig. 10) gives 30.22. This correction would bring the PNLF distance modulus in better (but not perfect) agreement with the surface brightness fluctuation (SBF) distance modulus (30.35 ± 0.2) reported by Tonry et al. (2001).

4. DISCUSSION

4.1. Can the NGC 4697 PN sample be contaminated?

Bright PNs play a significant role in the analysis of the last section. Is it possible that the brightest PNs in NGC 4697 are contaminated by compact HII regions such as those observed in Gerhard et al. (2002); Ryan-Weber et al. (2004)? The recent observations of Méndez et al. (2005) have shown that this cannot be so. These authors took spectra of 13/42 PNs in our bright subsample in NGC 4697 with FORS2@VLT; these have no detectable continuum and the line ratios of metal-rich PNs.

The same argument also shows that these bright PNs cannot be background emission line galaxies. Moreover, Ly alpha emission galaxies would come in at [OIII] magnitudes of $m_{5007} \gtrsim 26.2$ (see Fig. 4 of Aguerri et al. 2005), while the bright PNs in NGC 4697 have $m_{5007} \leq 26.2$.

Furthermore, one may wonder whether the bright PNs in NGC 4697 might simply be foreground objects which could be closer to us and hence brighter than the 'true' NGC 4697 PNs on which they would be superposed. Given that NGC 4697 is located in the southern extension of the Virgo cluster, known to contain an intra-
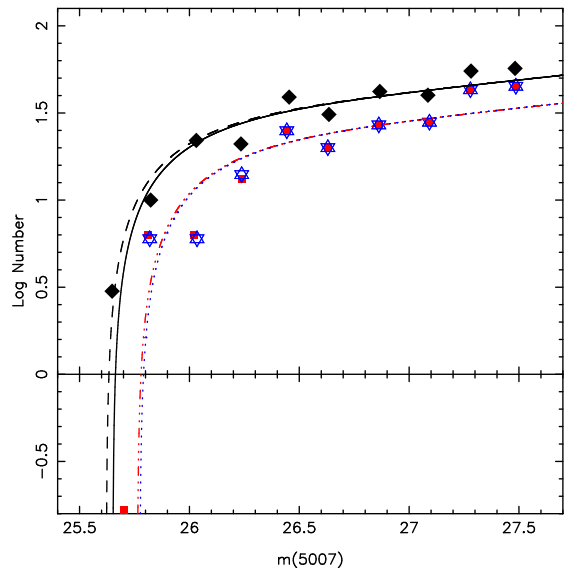

FIG. 10.— Distributions of PN magnitudes in NGC 4697. The PNLF for all PNs (black diamonds, dashed black line) is similar to the PNLF of Méndez et al. (2001) (black solid line). The red squares and χ^2-fitted dash-dotted line show the PNLF of the main population of PNs in the velocity range $-100\,\mathrm{km\,s^{-1}} \leq U \leq 200\,\mathrm{km\,s^{-1}}$, but with the bright PNs in the angular overdensity weighted only by 2/12 so that the angular distribution of the bright PNs becomes approximately uniform. The blue stars and χ^2-fitted blue dotted line show the PNLF in the same velocity range, but now with the 10 brightest PNs in the angular overdensity removed.

cluster population of PNs (Arnaboldi et al. 2002, 2004; Feldmeier et al. 2004), this possibility deserves to be considered. However, the following observational facts show that the bright PNs in NGC 4679 are not intracluster PNs (ICPNs). (1) NGC 4697 is in fact closer than the Virgo cluster. The PNLF from Méndez et al. (2001) places it at $10.5 \pm 1\,\mathrm{Mpc}$ (m-M= 30.1), while the distance modulus from the PNLF of M87 is m-M= 30.7 ± 0.1 (Ciardullo et al. 2002). Even if we discarded the entire brightest 0.3 mag of the NGC 4697 PNs, NGC 4697 would still be at 75% of the distance of M87. (2) The velocity dispersion of the bright and unrelaxed PNs in NGC 4697 is $\sim 170\,\mathrm{km\,s^{-1}}$, but varying azimuthally, while that of the fainter main population is $123\,\mathrm{km\,s^{-1}}$ (Table 2, Figs. 1, 5). Both are much smaller than the velocity dispersion of ICPNs in Virgo (Arnaboldi et al. 2004). The radial distribution of the bright population outside the incompleteness ellipse is concentrated towards the galaxy center and KS compatible (92%) with the radial distribution of the fainter PNs (see Fig. 4). Thus also the bright PNs in NGC 4697 are bound to the galaxy. (3) The surface density of PNs with $m_{5007} \leq 26.2$ is 0.58 PNs/arcmin^2, while the mean surface density of Virgo ICPNs is 0.02 PNs/arcmin^2, much smaller (Aguerri et al. 2005). This last argument also rules out significant contamination by chance superpositions of PNs even closer than NGC 4697.

We conclude that the bright PN population in NGC 4697 consists of genuine PNs, and that it is dynamically bound to the NGC 4697 system. The irregular angular distribution and kinematics of these PNs, by comparison with the fainter main population, show that they must belong to a separate stellar population not yet in dynamical equilibrium with NGC 4697.
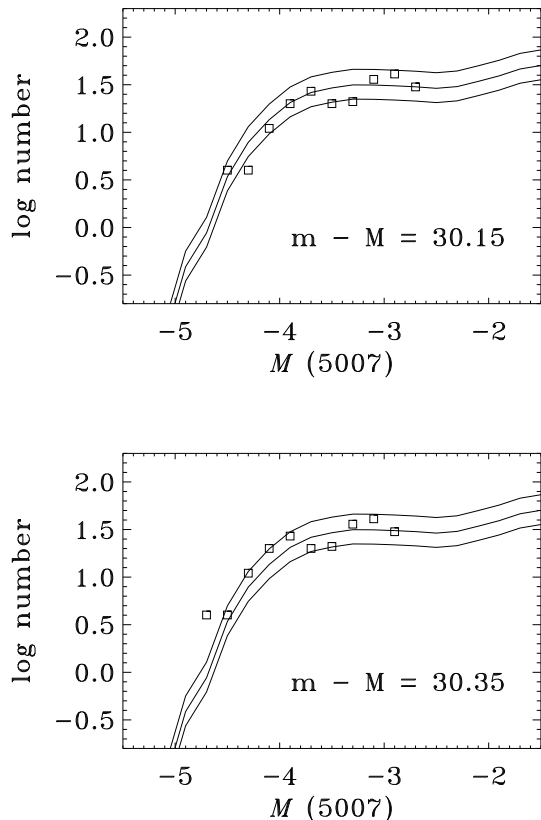
FIG. 11.— PNLF of NGC 4697 (squares), built from the main population PN sample (blue stars in Fig. 10) of 214 objects, binned into 0.2 mag intervals. The apparent magnitudes $m(5007)$ have been transformed into absolute magnitudes $M(5007)$ by adopting an extinction correction of 0.105 mag and distance moduli indicated in each plot. The three lines are PNLF simulations (Méndez & Soffner 1997). For a distance modulus 30.15 the brightest PNs are a bit too weak, therefore the distance must be increased. But 30.35 is clearly excessive. The best fit is for 30.2 or 30.25.

4.2. Comparison with other galaxies

PN samples as large as the one for NGC 4697 are still the exception. Yet to undertake the analysis described in Section 3 it was crucial to work with a complete sample of some 300 PNs. The PN.S project (Douglas et al. 2002) may lead to complete samples of similar size but as of now the typical sample sizes are $\lesssim 200$ (Romanowsky et al. 2003) and their magnitude distributions and completeness have not been studied. The only other elliptical galaxy with a comparable (even larger) sample is Cen A (Hui et al. 1995; Peng, Ford & Freeman 2004). A detailed analysis of the distribution of Cen A PNs in the magnitude–velocity plane is still pending, but Hui et al. (1993) analysed the PNLF in Cen A as a function of radius, based on narrow-band surveys. They concluded that no population effect on the PNLF bright cut-off could be seen, suggesting that the 0.3 mag difference between their main and outer halo samples was due to filter transmission uncertainties. Analysis of the large sample from Peng, Ford & Freeman (2004) will clarify whether the PNs in Cen A are consistent with one or more subpopulations. This will be particularly interesting because Cen A is believed to be the remnant of a galaxy merger, so one might expect PNs from both

the older stellar populations of the progenitors as well as from the stars formed in the subsequent interaction between them.

Without large kinematic samples, searches for PN subpopulations must be based on the PN luminosity distributions. The work of Jacoby, Ciardullo and collaborators cited in the Introduction has shown that the PNLF is remarkably uniform. However, there are exceptions: we recall that in the halo of M84 there exists a small population of overluminous PNs whose cutoff is 0.3 mag brighter than that of the main M84 population, but which appear nonetheless bound to the halo of M84 (Arnaboldi et al. 2004; Aguerri et al. 2005). They must therefore be intrinsically bright, due to some stellar population difference. In M87, the only overluminous PNs projected onto the galaxy for which velocities have been measured (Arnaboldi et al. 2004), have very large relative velocities with respect to M87. This is most naturally explained if these PNs have fallen into the deep potential well of M87 from far out in the cluster; this would again imply an intrinsic population difference. However, a larger kinematic sample in M87 is required to be certain.

The existence of the bright PN subpopulation in NGC 4697 implies some uncertainty in the PNLF cut-off luminosity for this galaxy. Depending on whether or not the azimuthally symmetric brightest PNs are part of the main population, the cut-off luminosity of the main PN population in NGC 4697 is fainter than that of the whole population by $\gtrsim 0.15$ mag (Figs. 10, 11). While this is consistent with the M84 result, is it also consistent with the systematic studies of PNLF distances? Ciardullo et al. (2002) have compared the PNLF and SBF distances, finding a distribution of residuals with a systematic offset by $\simeq 0.3$ mag, which they suggested is due to internal extinction effects, and with a FWHM of $\simeq 0.5$ mag. The offset has in the mean-time been reduced to $\simeq 0.15$ mag, following a revision of the SBF distance scale by Jensen et al. (2003). The width of this distribution is consistent with their determination of the observational errors in both methods. However, the offset we have determined for NGC 4697 is also consistent with the distribution of residuals in Ciardullo et al. (2002).

4.3. Origin of the PN population difference: a secondary, younger stellar population?

We have shown that a large fraction of the bright PNs in NGC 4697 belong to a secondary, dynamically young stellar population that is not well-mixed in the gravitational potential of the galaxy. Late infall of tidal structures (Zezas et al. 2003) or a merger with a smaller galaxy some time ago would be natural ways to add such an unmixed stellar component to NGC 4697. What physical population difference is correlated with this dynamical youth?

Méndez et al. (2005) show from their spectroscopic data for 13 bright PNs that these have near-solar metallicities. Of these 13 bright PNs, 6 are inside the incompleteness ellipse, one has no measured velocity, and 6 belong to our secondary population. Méndez et al. (2005) also use long-slit spectroscopy to show that the metallicity of the integrated stellar population within one effective radius has solar or higher metallicities. These observations make it unlikely that metallicity is the main

factor responsible for the different magnitude distributions of the main and secondary PN populations in NGC 4697.

Thus the more likely driver would appear to be an age difference, as suggested by Marigo et al. (2004) and as might generally be expected in an accretion event. Based on their result that the distribution of X-ray point sources in NGC 4697 does not follow the stellar light, Zezas et al. (2003) have argued that this is because these sources were formed several 10^8 years ago in tidal tails that are now falling back onto the galaxy. Note, however, that the integrated light in NGC 4697 shows no evidence of young stars with mean age < 7 Gyr (Méndez et al. 2005), so this younger component could not be luminous enough to contaminate the integrated light to the level measured. Also note that the observed increase of extinction in the PN envelope with PN core mass more than compensates for the increase of core luminosity with core mass, for bright PNe in local group galaxies (Ciardullo & Jacoby 1999), so that stars with ages below 1 Gyr may not reach the [OIII] luminosity at the PNLF cutoff. A secondary stellar population younger than 1 Gyr is therefore unlikely as well.

Recently, Ciardullo et al. (2005) have argued that the brightest PNs in the PNLF must have core masses of $\gtrsim 0.6\,M_\odot$, corresponding to main sequence masses of $\sim 2.2\,M_\odot$. They argue further that for such high-mass objects to occur in elliptical galaxies, these early-type galaxies would either have to contain a small, smoothly distributed component of young ($\lesssim 1$ Gyr age) stars, or more likely, that the bright PNs in these systems have evolved from blue straggler stars created through binary evolution. Their blue straggler model, due to the assumption of a fixed distribution of primary-to-secondary mass ratios for the initial binaries, predicts that older stellar populations produce fewer bright PNs per unit luminosity, as is observed, because the number of binary stars in a stellar population that can coalesce to $\sim 2.2\,M_\odot$ blue stragglers decreases with time.

If correct, this blue straggler model could also explain how the secondary population we found in NGC 4697 can contain a large fraction of the brightest PNs in this galaxy, provided that the stellar population corresponding to this secondary PN population is appreciably younger than the main stellar population, whose age is ~ 9 Gyr from optical spectroscopy (Trager et al. 2000). At the same time, this secondary stellar population must not be so young to violate either the constraints from the optical colours or from the envelope absorption - PN core mass correlation, i.e., must be older than ~ 1 Gyr. We can give an estimate for the effect of such an intermediate age population on the optical colours as follows. The secondary subpopulation traced by the bright and predominantly counterrotating PNs may contain $\sim 20\%$ of all PNs in the Complete sample for NGC 4697. A stellar population as blue as the bulge of M31 has a luminosity-specific PN density per unit L_B up to 5 times higher than the populations characteristic for old elliptical galaxies (Hui et al. 1993; Ciardullo et al. 2005). Thus the subpopulation corresponding to the secondary PN population in NGC 4697 would be expected to contain $\gtrsim 5\%$ of the blue luminosity of NGC 4697, spread over a large fraction of at least the E image. To detect this we need deep and accurate photometry.

The unmixed spatial and velocity distributions of the secondary PN population in NGC 4697 show that that this population is *dynamically young*, i.e, has not had time to phase-mix and come to dynamical equilibrium in the gravitational potential of NGC 4697. It may well be associated with tidal structures that were formed in a merger or accretion event $\sim 1 - 2$ Gyr ago, and that have now fallen back onto the galaxy, or be associated with a more recent merger/accretion with a red galaxy such as described in van Dokkum (2005). In a Universe in which structures form hierarchically, such secondary stellar populations might be quite common in ellipitical galaxies, but they would be difficult to see. The present work shows that studying their PN populations is one promising approach of looking for such secondary populations. However, large PN samples are required; most existing PN studies of early-type galaxies do not have the statistics for such an investigation. Moreover, in only a fraction of cases may there be enough asymmetry signal to detect with a few hundred PNs.

5. CONCLUSIONS AND IMPLICATIONS

We have analysed the magnitudes, kinematics and positions of a complete sample of 320 PNs in the elliptical galaxy NGC 4697 from Méndez et al. (2001). This data set is large enough for drawing statistically significant conclusions, and it does not suffer from detection incompletenesses in either magnitudes or radial velocities. We know of no systematic effects in the data that could explain our results. Our main conclusions are:

1. Bright and faint PNs in NGC 4697 have significantly different radial velocity distributions. The mean velocities of the faint and bright subsamples (co-rotating and ~ 0, respectively) and their velocity dispersions are different, with 94% and 99.3% confidence. Thus the PNs in NGC 4697 do not constitute a single population that is a fair tracer of the distribution of all stars.

2. The luminosity functions of the extreme counter-rotating subsample ($U < -100\,\mathrm{km\,s^{-1}}$) and of the main population (defined by $-100\,\mathrm{km\,s^{-1}} \leq U \leq 200\,\mathrm{km\,s^{-1}}$) are different with 99.7% confidence. The PNLF is therefore not universal.

3. Based on this, we suggest that there exist (at least) two PN populations in this galaxy. The secondary PN population in NGC 4697 is prominent in a subsample of counter-rotating PNs brighter than 26.2. The luminosity function of the entire extreme counterrotating sample may be a first approximation to the luminosity function of the secondary population.

4. The spatial distribution of bright PNs with $m(5007) < 26.2$ is different from that of the faint PNs. The bright PNs do not follow the azimuthal distribution of the optical light, show a left-right asymmetry, and have a positive mean radial velocity on both sides of the galaxy major axis, but zero velocity and larger dispersion on the minor axis. They are not in dynamical equilibrium in the potential of the galaxy. The fainter population has rotation properties more similar to the absorption

line velocities, with azimuthally constant dispersion.

5. Using both their kinematics and angular distribution, we can estimate a lower limit to the statistical fraction of bright PNs in the secondary population. Based on this we estimate that the bright cutoff of the main population is uncertain by ~ 0.15 mag.

Our results have two main implications for the use of PNs in extragalactic astronomy. First, for distance determinations with the PNLF, it may be important to understand how uniform the PN populations in the target galaxies are. From our analysis in NGC 4697 we estimate that unrecognized subpopulations of PNs in smaller samples than that in NGC 4697 may lead to variations of ~ 0.15 mag in the bright cutoff. This would correspond to distance errors of some 10%, which, although a minor effect, could be significant in some cases. It will be necessary to verify how frequently such subpopulations occur in elliptical galaxies. We recall that also in the halo of M84 there exists a small population of overluminous PNs whose cutoff is 0.3 mag brighter than that of the main M84 population, but which appear nonetheless bound to the halo of M84 (Arnaboldi et al. 2004; Aguerri et al. 2005).

The second implication concerns the use of PNs as tracers for the angular momentum and gravitational potentials of elliptical galaxies. Our analysis has shown that in NGC 4697 the bright PNs do not trace the distribution and kinematics of stars and are not in dynamical equilibrium in the gravitational potential of the galaxy. The fainter PNs look more regularly distributed but may also contain a fraction of PNs that belongs to this out-of-equilibrium population. Clearly therefore, mass determinations based on PN kinematics will in future require careful study of the PN samples being used, not only to verify that these PNs are in dynamical equilibrium, but also to test for different dynamical components. Even if in equilibrium, a younger population of stars may be more flattened or have a steeper fall-off than the main body of the elliptical galaxy. If the PNs from this population are indeed somewhat brighter than the main population, one can recognize such differences from their lower velocity dispersion or different radial density profile. However, deep observations and large PN samples will be required.

REFERENCES

Aguerri, J.A.L. et al. 2005, AJ, 129, 2585

Arnaboldi, M. et al. 1998, ApJ, 507, 759

Arnaboldi, M. et al. 2002, AJ, 123, 760

Arnaboldi, M., Gerhard, O.E., Aguerri, J.A.L., Freeman, K.C., Napolitano, N., Okamura, S., Yasuda, N., et al. 2004, ApJ, 614, L33

Binney, J., Davies, R.L., & Illingworth, G.D. 1990, ApJ, 361, 78

Carter, D. 1987, ApJ, 312, 514

Ciardullo, R., & Jacoby, G.H. 1999, ApJ, 515, 191

Ciardullo, R. 2003, in Stellar Candles for the Extragalactic Distance Scale, ed. D. Alloin & W. Gieren, Lect Notes Phys., 635, 243

Ciardullo, R. et al. 2002, ApJ, 577, 31

Ciardullo, R., Jacoby, G.H., Ford, H.C., & Neill, J.D. 1989, ApJ, 339, 53

Ciardullo, R., Sigurdsson S., Feldmeier, J.J., & Jacoby, G.H. 2005, ApJ, 629, 499

Dejonghe, H. et al. 1996, A&A, 306, 363

Dekel, A., Stoehr, F., Mamon, G.A., Cox, T.J., Novak, G.S., & Primack, J.R. 2005, Nature, astro-ph/0501622

Dopita, M.A., Jacoby, G.H., & Vassiliadis, E. 1992, ApJ, 389, 27

Douglas, N. et al. 2002, PASP, 114, 1234

Feldmeier, J. J., Ciardullo, R., & Jacoby, G. H. 1998, ApJ, 503, 109

Feldmeier, J. J., Ciardullo, R., Jacoby, G. H., & Durrell, P. R. 2004, ApJ, 615, 196

Ferrarese, L. et al. 2000, ApJ, 529, 745

Gerhard, O. et al. 2002, ApJ, 580, L121

Gerhard, O., Arnaboldi, M., Freeman, K.C., Kashikawa, N., Okamura, S., & Yasuda, N., 2005, ApJ, 621, L93

Goudfrooij, P., et al. 1994, AAS, 104, 179

Hui, X., Ciardullo, R., & Jacoby, G.H. 1995, ApJ, 414, 463

Hui, X., Ford, H.C., Freeman, K.C., & Dopita, M.A. 1995, ApJ, 449, 592

Jacoby, G.H. 1997, in The Extragalctic Distance Scale, Space Telescope Science Institute Series, ed. M. Livio (Cambridge University Press), 197

Jacoby, G.H. 1989, ApJ, 339, 39

Jacoby, G.H., Ciardullo, R., & Ford, H.C. 1990, ApJ, 356, 332

Jensen, J.B., et al.2003, ApJ, 583, 712

Marigo, P., Girardi, L., Weiss, A., Groenewegen, M.A.T., & Chiosi, C. 2004, A&A, 423, 995

Méndez, R.H. 1999, in Post-Hipparcos Cosmic Candles, ed. A. Heck & F. Caputo (Dordrecht: Kluwer), 161

Méndez, R.H., & Soffner, T. 1997, A&A, 321, 898

Méndez, R.H., Kudritzki, R.P., Ciardullo, R., & Jacoby, G.H. 1993, A&A, 275, 534

Méndez, R.H. et al. 2001, ApJ, 563, 135

Méndez, R.H. et al. 2005, ApJ, 627, 767

Merritt, D., & Saha, P. 1993, ApJ, 409, 75

Peng, E., Ford, H.C., & Freeman, K. C. 2004, ApJ, 602, 685

Romanowsky, A.J., et al. 2003, Science, 301, 1696

Ryan-Weber, E.V., et al. 2004, AJ, 127, 1431

Saglia, R.P., Kronawitter, A., Gerhard, O.E., & Bender, R., 2000, AJ, 119, 153

Sansom, A.E., Hibbard, J.E., & Schweizer, F. 2000, AJ, 120, 1946

Sarazin, C.L., Irwin, J. A., & Bregman J.N. 2000, ApJ, 544, L101

Scorza, C., & Bender, R. 1995, A&A, 293, 20

Tonry, J.L., et al. 2001, ApJ, 546, 681

Trager, S.C., Faber, S.M., Worthey, G., & González, J.J. 2000, AJ, 119, 1645

van Dokkum, P.G. 2005, AJ, submitted, astro-ph/0506661

Zezas, A., Hernquist, L., Fabbiano, G., & Miller, J. 2003, ApJ, 599, L73